



Contents lists available at ScienceDirect

Spectrochimica Acta Part A: Molecular and Biomolecular Spectroscopy

journal homepage: www.elsevier.com/locate/saaNew 15-membered tetraaza (N_4) macrocyclic ligand and its transition metal complexes: Spectral, magnetic, thermal and anticancer activity

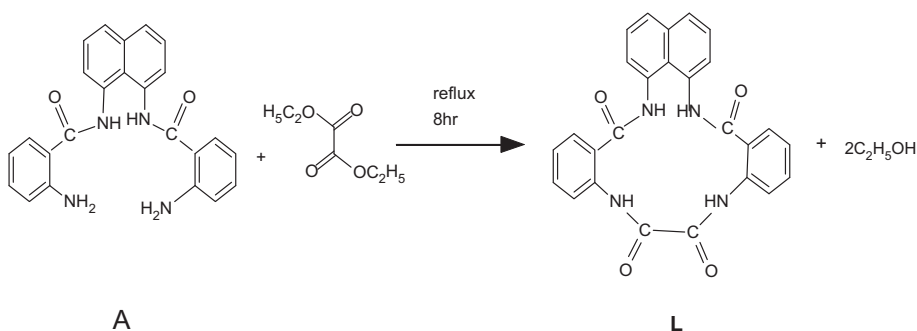
Hanaa A. El-Boraey*, Ohyla A. EL-Gammal

Department of Chemistry, Faculty of Science, El-Menoufia University, Shebin El-Kom, Egypt

HIGHLIGHTS

- Novel metal complexes of (N_4) macrocyclic ligand have been synthesized and characterized.
- Analytical, spectral and thermal data confirm the structure of the compounds.
- *In vitro* antitumor activity shows that the obtained compounds are potent anticancer agents.

GRAPHICAL ABSTRACT



ARTICLE INFO

Article history:

Received 30 August 2014
 Received in revised form 29 October 2014
 Accepted 5 November 2014
 Available online 26 November 2014

Keywords:

Tetraazamacrocyclic
 Macrocyclic metal complexes
 Spectral studies
 Antitumor activity
 IC_{50}

ABSTRACT

Novel tetraamidemacrocyclic 15-membered ligand [L] i.e. naphthyl-dibenzo[1,5,9,12]tetraazacyclopentadecine-6,10,11,15-tetraone and its transition metal complexes with Fe(II), Co(II), Ni(II), Cu(II), Ru(III) and Pd(II) have been synthesized and characterized by elemental analysis, spectral, thermal as well as magnetic and molar conductivity measurements. On the basis of analytical, spectral (IR, MS, UV–Vis, 1H NMR and EPR) and thermal studies distorted octahedral or square planar geometry has been proposed for the complexes. The antitumor activity of the synthesized ligand and some complexes against human breast cancer cell lines (MCF-7) and human hepatocarcinoma cell lines (HepG2) has been studied. The complexes (IC_{50} = 2.27–2.7, 8.33–31.1 $\mu g/mL$, respectively) showed potent antitumor activity, towards the former cell lines comparable with their ligand (IC_{50} = 13, 26 $\mu g/mL$, respectively). The results show that the activity of the ligand towards breast cancer cell line becomes more pronounced and significant when coordinated to the metal ion.

© 2014 Elsevier B.V. All rights reserved.

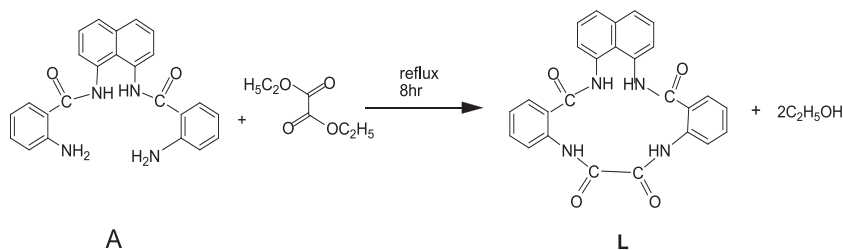
Introduction

The design and synthesis of macrocycles and their metal complexes represent an active area of research due to their widespread applications in biology, supra-molecular chemistry, new materials [1–14], etc. These rings can accommodate a variety of metal ions depending on the cavity size, metal ion, and ring structure, for transition metal ions, features such as the nature and magnitude

of crystal-field effects play also an important role [15,16]. The interest in macrocyclic complexes especially those with polydentate ligands stems from the chemical properties that the macrocyclic ligands bring to the complexes as well as the variety of geometrical forms available and the possible encapsulation of the metal ion [17,18]. Complexes with polyazamacrocyclic ligands have remained a focus of scientific attention and have potential applications in different areas [7,10,19,20]. One class of these macrocycles is those incorporating amide groups. The amide groups can bind with different metal ions via nitrogen and/or oxygen atoms [1,2,21–24]. These compounds not only can act as hydrogen-bonding host molecules

* Corresponding author. Tel.: +20 111 7532777; fax: +20 48 2235689.

E-mail address: helboraey@yahoo.com (H.A. El-Boraey).



Scheme 1. Synthetic route for the preparation of macrocyclic ligand (L).

but also can form macrocyclic rotors [25]. Also, Macrocylic amides are ubiquitous in biochemistry, because they provide the linkages that held together two of the most important types of biopolymers, nucleic acids and proteins [22,26]. Moreover, macrocylic amides have potential applications in electrophosphorescence devices (EL) and homogenous catalysis [27]. Very recently we have synthesized and characterized a new macrocylic ligand and its transition metal complexes [8]. This ligand represents a 15-membered (N_5) ligand i.e. 1,5,8,12-tetraaza-3,4:9,10-dibenzo-6-ethyl-7-methyl-1,12-(2,6-pyrido)cyclopentadecan-5,7 diene-2,11-dione. The ligand and its transition metal complexes show an important biological activity as anticancer agents. As a continuation to our work we report herein the synthesis, spectroscopic characterization and anticancer activity of Fe(II), Co(II), Ni(II), Cu(II), Ru(III), Pd(II) complexes with new tetraamidemacrocyclic 15-membered (N_4) ligand i.e. naphthylidibenzo[1,5,9,12]tetraazacyclopentadecine-6,10,11,15-tetraone. These complexes have been characterized with the help of various physicochemical techniques. Further the antitumor activity against human breast cancer cell line MCF-7, and human hepatocarcinoma cell HepG2 *in vitro* were detected.

Experimental

Materials and methods

All chemicals used in the synthesis were of reagent grade and used as submitted from Aldrich without further purification. Isoatoxal anhydride, 1,8-diaminonaphthalene and diethyl oxalate were purchased from Sigma Aldrich Chemical Company and used as received.

Synthesis of the starting material

The starting material (A) has been synthesized as previously reported for similar compounds [1,8,28]. A mixture of 1H-benzod[1,3]oxazine-2,4-dione (1 g, 6 mmol) with 1,8-diaminonaphthalene (0.48 g, 3 mmol) (2:1 M ratio) in hot distilled water was stirred at 60 °C for about 1 h. Heating on water bath was continued till the effervescence of CO_2 gas ceased. The reaction mixture was allowed to stand overnight. The brown solid precipitate was collected by filtration, washed with hot water and dried in vacuum. Recrystallization from ethanol gave brown crystals of 2-amino-N-[2-(2-amino-benzoylamino)-naphthyl]-benzamide (A) (Scheme 1). Color: brown, yield: 1.00 g (100%), m.p.: 120 °C. Anal. Calc.% for $C_{24}H_{20}N_4O_2 \cdot 1\frac{1}{2}H_2O$ (MW: 423): C 68.08, H 5.4, N 13.24. Found: % C 67.83, H 5.33, N 12.51. Selected IR data (KBr, cm^{-1}): 3466 $\nu(OH)$, 3371 $\nu(NH_2)$, 1630 $\nu(C=O)$, 1503 $\nu[\nu(C-N) + \delta(N-H)]$, 1240 $\nu(C-N)$, 752 $\phi(C=O)$. 1H NMR (DMSO- d_6 , ppm) δ = 6.603–8.64 (Ar, H), δ = 6.577–6.579 (Ar- NH_2), δ = 12.065 (NH- amide). Mass spectrum (EI, m/z): Calc. M = 396, Found: 395 (M-H) $^+$.

Synthesis of ligand (L)

0.5 g (1 mmol) of compound (A) in acetone was refluxed with 0.22 g (0.2 ml) of diethyl oxalate in ethanol in molar ratio (1:1)

for 8 h. The brown solid precipitate formed was collected by filtration and washed several times with cold ethanol and dried under vacuum.

Synthesis of the metal complexes

All the metal complexes (Scheme 2) were prepared as follows: 0.5 g of the ligand was dissolved in 50 mL acetone. To this solution 20 mL ethanolic solution of different metal salt was added dropwise in molar ratio 1:1 (metal:ligand). The reaction mixture was stirred under reflux whereupon the complexes precipitated. The precipitated solid complex was separated from the solution by filtration, purified by washing several times with ethanol and then dried under vacuum at room temperature.

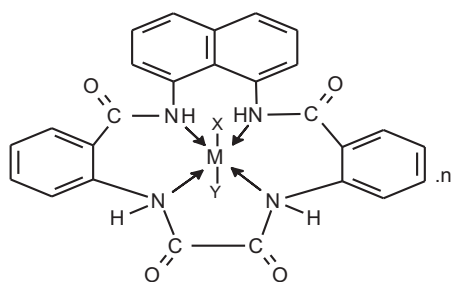
Physical measurements

The elemental analyses (C,H,N) were performed at Microanalytical Center, Cairo University Giza, Egypt using CHNS-932 (LECO) Vario Elemental Analyzer.

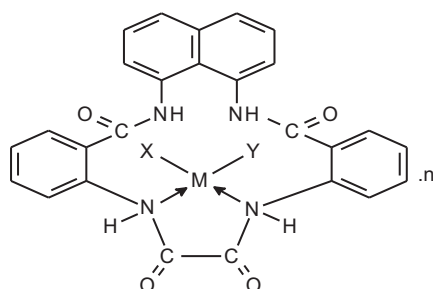
Metals and halide analyses were estimated using standard methods [29,30]. Electrospray mass spectra (ESI) for the complexes were performed at the National Research Center, Egypt by the Thermo Electron Corporation. The electron impact mass spectrum (EI) for the ligand was run on Shimadzu-QP 2010 plus Mass Spectrometer, Microanalytical Laboratory, Faculty of Science, Cairo University, Egypt. The Fourier Transform Infrared (FTIR) measurements were performed (4000–400 cm^{-1}) in KBr discs using Neneux-Nicolite-640-MSA FT-IR, Thermo-Electronics Co. The UV-visible absorption spectra were measured in DMF using 4802 UV/vis double beam spectrophotometer. The 1H NMR spectrum was recorded in DMSO- d_6 using Varian Gemini 200 NMR spectrophotometer at 300 MHz. The electron paramagnetic resonance (EPR) spectra were recorded using a Varian E-109C model X-band spectrometer. The magnetic field modulation frequency was 100 kHz and the microwave power was around 10 mW. Molar conductivities were measured in DMF solution of the complexes (10^{-3} M) using a CON 6000 conductivity meter, Cyberscan, Eutech Instruments. Magnetic susceptibilities of the complexes were measured by the modified Gouy method at room temperature using Magnetic Susceptibility Johnson Matthey Balance. The effective magnetic moments were calculated using the relation $\mu_{eff} = 2.828(\chi_m T)^{1/2}$ B.M., where χ_m is the molar magnetic susceptibility corrected for diamagnetism of all atoms in the compounds using Selwood and Pascal's constants. Thermal analysis (TG/DTG) was obtained out by using a Shimadzu DTA/TG-50 Thermal analyzer with a heating rate of 10 °C/min in nitrogen atmosphere with a following rate 20 mL/min in the temperature range 30–800 °C using platinum crucibles.

Biological tests

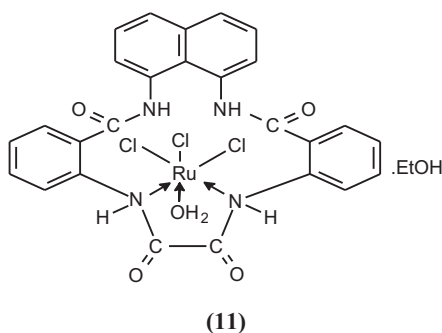
The cytotoxicity of the compounds was tested at the National Cancer Institute, Cairo University Egypt by SRB assay using the method of Skehan et al. [31]. Cells were plated in 96-multiwell



No	M	X	Y	n
(1)	Fe(III)	Cl	OH	H ₂ O
(2)	Co(II)	OAc	OAc	2H ₂ O
(3)	Ni(II)	Cl	OH	EtOH
(4)	Ni(II)	NO ₃	NO ₃	½EtOH
(5)	Ni(II)	OAc	OAc	3H ₂ O
(7)	Cu(II)	Br	OH	EtOH
(8)	Cu(II)	NO ₃	OH	EtOH



No	M	X	Y	n
(6)	Cu(II)	Cl	Cl	H ₂ O.½EtOH
(9)	Cu(II)	OAc	OAc	2H ₂ O
(10)	Cu(II)	ClO ₄	OH	3H ₂ O
(12)	Pd(II)	Cl	Cl	1½ H ₂ O



Scheme 2. Suggested structure of the compounds (1–12).

plate (10^4 cells/well) for 24 h before treatment with the compounds to allow attachment of cell to the wall of the plate. Different concentrations of the compound under test (0, 2.5, 5, 10, 20 $\mu\text{g}/\text{mL}$) added to the cell monolayer triplicate wells were prepared for each individual dose. Monolayer cells were incubated with the compounds for 48 h at 37 °C and in atmosphere of 5% CO₂. After

48 h, cells were fixed, washed and stained with Sulfo-Rhodamine-B stain. Excess stain was washed with acetic acid and attached stain was recovered with Tris EDTA buffer. Color intensity was measured in an ELISA reader. The relation between surviving fraction and drug concentration is plotted to get the survival curve of each tumor cell line after the specified compound.

Results and discussion

The reaction of (A) with diethyloxalate gives the expected tetraamidemacrocyclic compound, L. This ligand represents a 15-membered (N₄) macrocyclic molecule (Scheme 1). The macrocyclic ligand and its metal complexes are air stable at room temperature, non-hygroscopic. The elemental, spectral, magnetic and thermal analysis data (Tables 1–5) are consistent with their proposed molecular formulae. The elemental analyses show that all complexes are formed in 1 M:1 L molar ratio. It should be noted that many attempts have failed to crystallize suitable single crystals for X-ray analysis for any of complexes, due to their partial solubility in common organic or mixed solvents. However, they are soluble in polar solvents such as DMF/DMSO. The conductance measurements, recorded for 10^{-3} M solution of the metal complexes in DMF, are listed in Table 1. All complexes are non-conducting and the measured molar conductance ranged from 27 to $3 \Omega^{-1} \text{cm}^2 \text{mol}^{-1}$ indicating their neutrality [32,33].

FT-IR

The preliminary identification regarding formation of the complexes, were obtained from IR spectral findings (Table 2). In general, the IR spectrum of the free ligand shows strong bands at 3376, 1625, 1514, 1296, and 754 cm^{-1} , which are attributed to the stretching frequencies of NH, amide-I $\nu(\text{C}=\text{O})$, amide-II [$\nu(\text{C}-\text{N}) + \delta(\text{N}-\text{H})$], amide-III $\nu(\text{C}-\text{N})$ and amide-IV $\phi(\text{C}=\text{O})$ bands, respectively [1,34–36], which support to macrocyclic nature of the ligand. The IR spectrum also shows two peaks at 2930, 2869 cm^{-1} , attributed to Intra- and/or intermolecular hydrogen bonds. On complexation, the lowering of amide-I $\nu(\text{C}=\text{O})$ frequency value in complexes (1–5,7,8) (1623–1603 cm^{-1}) indicating the coordination of the four amide nitrogen. However, the stretching frequency of the amide-I $\nu(\text{C}=\text{O})$ group in the complexes (6,9,10–12) was observed in two separate regions. The former region was observed at (1616–1606 cm^{-1}) which is lower than the amide-I of the free ligand (1625 cm^{-1}). The latter region was observed at 1652–1642 cm^{-1} which is higher than the stretching frequency of the free ligand. The latter region may be due to the presence of uncoordinated amide-I $\nu(\text{C}=\text{O})$ group. A further evidence for these coordination modes is the appearance of new band at 470–408 cm^{-1} due to $\nu(\text{M}-\text{N})$ stretching vibrations [2,11]. The IR spectra of the complexes also show that the amide II and amide III occur at 1514, 1296 cm^{-1} in the free ligand, are slightly shifted to lower or higher frequency (Table 2) supporting coordination through the amide nitrogen atoms [1]. Aquo and hydroxo complexes exhibit a strong as well as broad band at 3460–3246 cm^{-1} due to $\nu(\text{OH})$ vibration. This observation has been further confirmed by the appearance of new medium intensity band in the 501–571 cm^{-1} region, assignable to $\nu(\text{M}-\text{O})$ [37]. Further, the IR spectra of the complexes show the bands due to coordinated anions. The nitrate complexes (4,8) show the bands at 1383 cm^{-1} (ν_5), 1295–1296 cm^{-1} (ν_1), 1048–1051 cm^{-1} (ν_2) and 823–832 cm^{-1} (ν_3). The value of $\Delta(\nu_5-\nu_1)$, i.e., 88–87 cm^{-1} suggests the monodentate coordination of NO₃⁻ ions [38]. The presence of coordinated nitrate is also supported by conductance measurements (Table 1). The IR spectra of acetato complexes (2,5,9) display two bands at 1585 and 1367–1388 cm^{-1} . The energy separation between $\nu_{\text{asym}}(\text{COO})$ and $\nu_{\text{sym}}(\text{COO})$ is found to

Table 1
Analytical and physical data for the macrocyclic ligand and its complexes.

No	Compound	Color	Yield (%)	M. Wt	D.T/°C	Analysis: calc. (found) (%)					(A _m) ^a
						C	H	N	M	X	
	L = C ₂₆ H ₁₈ N ₄ O ₄ ·H ₂ O	Brown	35	468	200	66.66 (66.95)	4.27 (3.95)	11.96 (12.49)	–	–	–
1	[FeCl(OH)]·H ₂ O	Black	60	577.3	150	54.14 (54.21)	3.64 (3.45)	9.72 (9.98)	9.67 (9.3)	6.15 (5.9)	26
2	[CoL(OAc) ₂]·2H ₂ O	Brown	108	662.9	147	54.31 (53.35)	4.22 (4.3)	8.44 (8.9)	8.88 (9.42)	–	3
3	[NiLCl(OH)]·EtOH	Black	83	607.2	225	55.33 (56.35)	4.11 (3.97)	9.22 (9.96)	9.67 (9.7)	5.85 (5.9)	27
4	[NiL(NO ₃) ₂]·½EtOH	Brown	40	655.7	190	49.41 (50.1)	3.20 (3.09)	12.81 (12.34)	8.95 (9.39)	–	20
5	[NiL(OAc) ₂]·3H ₂ O	Brown	94	680.7	190	52.88 (52.55)	4.41 (4.3)	8.23 (8.71)	8.62 (8.81)	–	7
6	[CuLCl ₂]·H ₂ O·½EtOH	Black	80	626	220	51.75 (50.91)	3.67 (3.11)	8.95 (8.92)	10.14 (9.52)	11.34 (11.53)	7
7	[CuLBr(OH)]·EtOH	Dark-brown	100	656.5	250	51.18 (51.66)	3.80 (2.82)	8.53 (9.25)	9.67 (10.58)	12.18 (12.33)	9
8	[CuL(NO ₃)(OH)]·EtOH	Black	88	638.5	135	52.62 (52.92)	3.91 (3.47)	10.96 (11.53)	9.95 (10.16)	–	26
9	[CuL(OAc) ₂]·2H ₂ O	Dark-brown	100	667.5	230	53.93 (54.08)	4.19 (3.79)	8.38 (9.3)	9.51 (9.50)	–	14
10	[CuLClO ₄ (OH)]·3H ₂ O	Dark-brown	90	684	–	45.61 (45.3)	3.07 (3.37)	8.18 (7.54)	9.28 (8.89)	14.55 (13.93)	22
11	[RuLCl ₃ (H ₂ O)]·EtOH	Black	100	721.5	260	46.56 (46.95)	3.6 (3.31)	7.76 (7.51)	13.9 (13.46)	14.76 (14.2)	15
12	[PdLCl ₂]·1½H ₂ O	Gray	98	654	230	47.67 (48.54)	3.2 (3.5)	8.56 (8.65)	16.49 (16.73)	10.8 (10.8)	14

^a Ω⁻¹ cm² mol⁻¹ DMF solutions (10⁻³ M), X: Halogen.**Table 2**
Important IR spectral bands (cm⁻¹)^a of the macrocyclic ligand and its complexes.

No	Compound	ν OH/NH	Amide bands				ν (M-O)	ν (M-N)	(NO ₃ ⁻ , OAc ⁻ , ClO ₄ ⁻)
			I	II	III	(IV)			
	L = C ₂₆ H ₁₈ N ₄ O ₄ ·H ₂ O	3376(b)	1625(b)	1514(m)	1296(m)	754(s)	–	–	
1	[FeLCl(OH)]·H ₂ O	3417(b)	1623(b)	1512(m)	1263(vb)	756(s)	476(s)	409(s)	
2	[CoL(OAc) ₂]·2H ₂ O	3383(s)	1618(m)	1510(m)	1316(w)	756(s)	502(br)	421(m)	
3	[NiLCl(OH)]·EtOH	3318(b)	1608(w)	1524(s)	1296(m)	754(s)	519(w)	447(m)	
4	[NiL(NO ₃) ₂]·½EtOH	3422(b)	1616(b)	1519(s)	1295(w)	756(s)	525(w)	430(w)	
5	[NiL(OAc) ₂]·3H ₂ O	3393(b)	1618(b)	1506(s)	1298(m)	754(s)	519(w)	441(w)	
6	[CuLCl ₂]·H ₂ O·½EtOH	3431(s)	1651(m), 1609(m)	1520(s)	1296(m)	756(s)	501(s)	409(m)	
7	[CuLBr(OH)]·EtOH	3422(vb)	1608(w)	1515(s)	1296(m)	754(s)	522(w)	451(w)	
8	[CuL(NO ₃)(OH)]·EtOH	3426(b)	1614(b)	1516(m)	1296(w)	754(m)	543(w)	437(m)	
9	[CuL(OAc) ₂]·2H ₂ O	3443(b)	1652(m), 1616(w)	1511(s)	1296(m)	755(s)	505(m)	436(m)	
10	[CuLClO ₄ (OH)]·3H ₂ O	3421(vb)	1646(vb), 1610(vb)	1515(s)	1298(m)	755(s)	503(s)	431(w)	
11	[RuLCl ₃ (H ₂ O)]·EtOH	3426(b)	1606(vb)	1523(m)	1293(b)	754(s)	571(w)	470(m)	
12	[PdLCl ₂]·1½H ₂ O	3426(m)	1642(m), 1604(s)	1524(vs)	1297(m)	756(vs)	593(w)	448(w)	

^a vb, very broad; s, strong; m, medium; w, weak; b, broad; v, stretching.**Table 3**
Electronic spectral data (nm) and magnetic moment (B.M.) of the metal complexes.

No	Compound	λ _{max} (nm)	μ _{eff} (B.M.)
1	[FeLCl(OH)]·H ₂ O	530 ^a , 350 ^c , 260 ^d	4.76
2	[CoL(OAc) ₂]·2H ₂ O	520 ^a , 350 ^c , 260 ^d	4.9
3	[NiLCl(OH)]·EtOH	520 ^a , 340 ^c , 260 ^d	2.13
4	[NiL(NO ₃) ₂]·½EtOH	530 ^a , 340 ^c , 270 ^d	2.8
5	[NiL(OAc) ₂]·H ₂ O	540 ^a , 340 ^c , 260 ^d	2.8
6	[CuLCl ₂]·H ₂ O·½EtOH	700 ^a , 530 ^a , 320 ^c , 250 ^d	2.005
7	[CuLBr(OH)]·EtOH	520 ^a , 370 ^c , 250 ^d	2.1
8	[CuL(NO ₃)(OH)]·EtOH	530 ^a , 375 ^c , 250 ^d	2.08
9	[CuL(OAc) ₂]·2H ₂ O	700 ^a , 500 ^a , 360 ^c , 266 ^d	2.06
10	[CuLClO ₄ (OH)]·3H ₂ O	700 ^a , 530 ^a , 490 ^b , 320 ^c , 260 ^d	2.01
11	[RuLCl ₃ (H ₂ O)]·EtOH	550 ^a , 333 ^c , 278 ^d	1.88
12	[PdLCl ₂]·1½H ₂ O	600 ^a , 450 ^b , 345 ^c , 266 ^d	dia

^a d-d transition.^b LMCT.^c n → π*.^d π → π*.

be >144 cm⁻¹, and this indicates the monodentate nature of the acetate ion [18,37]. In complex (**10**), the peak around 1107 cm⁻¹ is splitted, which clearly explains the presence of coordinated perchlorate ion [39]. Therefore, and according to the IR spectra, it is concluded that the macrocyclic ligand behaves as a neutral quadridentate one, with the lone electron pair of four amide nitrogen atoms in complexes (**1–5,7,8**), while in complexes (**6,9,10–12**) the ligand behaves as a

bidentate one with the electron pair of two amide nitrogen atoms only.

Mass and ¹H NMR spectral studies

The electron impact (EI) mass spectrum of the ligand (Fig. 1) gives a molecular ion peak at m/z = 450 amu (Calc. m/z = 450). The spectrum also shows important fragment ions at: m/z 74 for [C₆H₅ – 3H]⁺, 103 for [C₇H₅O + 2H]⁺, 118 for [C₇H₅NO – H]⁺, 156 for [C₁₀H₈N₂]⁺, 277 for [C₁₇H₁₇N₃O + 2H]⁺, 395 for [C₂₄H₁₈N₄O₂ – H]⁺. The ¹H NMR spectrum of the ligand (Fig. 1S) was recorded in DMSO-d₆ solution. The spectrum displayed signal at δ (6.59–8.61 ppm) assigned to aromatic ring protons and signal at ca. δ (12.50 ppm) assigned to amide protons. Also ¹H NMR spectrum of [PdLCl₂]·1½H₂O complex (**12**) (Fig. 2S) was recorded in DMSO-d₆. The spectrum showed similar signals as for the ligand, but the position of the amide proton signal in the complex is downfield (11.88 ppm) in comparison with the free ligand (12.50 ppm), indicating the involvement of the amide group in chelation [8]. Thus, the ¹H NMR results support the assigned geometry.

Mass spectra of complexes

Mass spectra provide additional structural information about the analyzed species. The ESI-MS of complexes (**6,12**) (Fig. 2) show molecular ion peak at m/z = 626, 656 amu corresponding to [CuLCl₂]H₂O·½EtOH (**6**), [PdLCl₂]·1½H₂O + 2H (**12**) (calculated

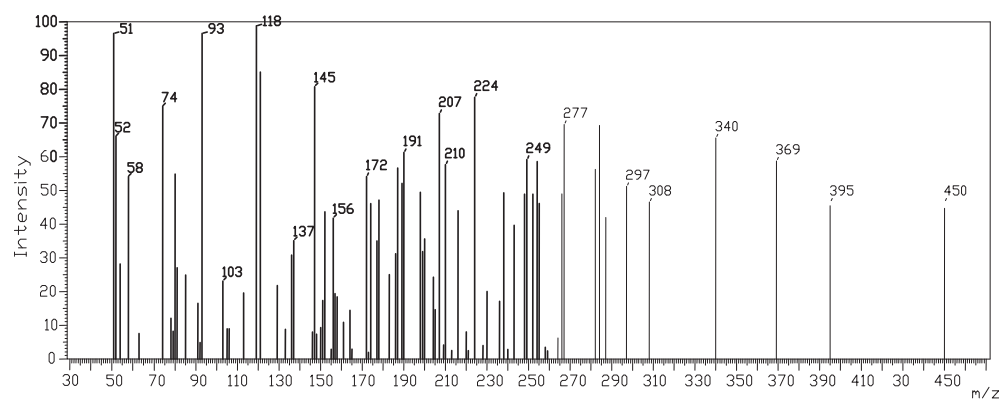
Table 4
EPR spectral data of Cu(II) complexes.

No	Complex	g_{\parallel}	g_{\perp}	g_{av}	G	$A_{\parallel} E^{-4} \text{ cm}^{-1}$	$A_{\perp} E^{-4} \text{ cm}^{-1}$	α^2	β^2	γ^2	f (cm)	K_{\parallel}	K_{\perp}	K
6	[CuCl ₂].H ₂ O.½EtOH	2.195	2.0335	2.0873	5.8	163	47.46	0.6986	0.9218	0.8345	128.5	0.644	0.583	0.36516
7	[CuBr(OH)].EtOH	2.195	2.0425	2.0933	4.58	–	–	–	–	–	–	–	–	–
8	[CuL(NO ₃)(OH)].EtOH	2.167	2.039	2.0816	4.28	–	–	–	–	–	–	–	–	–
9	[CuL(OAc) ₂].2H ₂ O	2.110	2.0335	2.0758	4.8	161	43	0.67166	0.8635	0.9138	127.65	0.5800	0.6138	0.602
10	[CuLClO ₄ (OH)].3H ₂ O	2.2237	2.0335	2.095	6.6	171	37.86	0.7278	0.977	0.8453	116.94	0.7114	0.6144	0.4203

$$g_{av} = \frac{2g_{\parallel} + g_{\perp}}{3}, \quad K^2 = \frac{2K_{\parallel}^2 + K_{\perp}^2}{3}$$

Table 5
Thermal data of the complexes.

No	Compound	Temp/°C		Wt. loss calc. (found)%	Reaction	Leaving species
		DTG	TG			
1	L = C ₂₆ H ₁₈ N ₄ O ₄ .H ₂ O	52	30–100	4.00(4.15)	(i) ^a	–H ₂ O
		202,335,586	200–650	96.00(95.85)	(ii) ^d	Decomp.
1	[FeLCl(OH)].H ₂ O	42	30–77	3.12(3.06)	(i) ^a	–H ₂ O
		162,354,386	150–477	87.22 (87.35)	(ii) ^d	Decomp.
2	[CoL(OAc) ₂].2H ₂ O	49	30–147	5.43(5.35)	(i) ^a	–2H ₂ O
		156,268,299	147–190	82.93(82.17)	(ii) ^d	Decomp.
3	[NiLCl(OH)].EtOH	53	30–92	12.5 (12.44)	(i) ^b	–EtOH
		306,374,529	200–559	7.57(7.66)	(ii) ^d	Decomp.
4	[NiL(NO ₃) ₂].½EtOH	61	30–85	9.66(9.6) ^c	(i) ^b	–Ni
		410,562	190–556	3.51(3.2)	(ii) ^d	–½EtOH
5	[NiL(OAc) ₂].3H ₂ O	57	30–148	87.54 (87.67)	(i) ^b	Decomp.
		204,339,380	190–445	8.95 (7.2) ^c	(ii) ^d	–Ni
6	[CuLCl ₂].H ₂ O.½EtOH	46	30–78	7.9(7.43)	(i) ^a	–3H ₂ O
		285,490	220–550	81.38(81.13)	(ii) ^d	Decomp.
7	[CuLBr(OH)].EtOH	56	30–132	10.97(11.29) ^c	(i) ^{a+b}	–(H ₂ O + ½EtOH)
		274,405,560	250–577	83.9(84.06)	(ii) ^d	Decomp.
8	[CuL(NO ₃)(OH)].EtOH	52	30–132	10.22(10.5) ^c	(i) ^b	–EtOH
		132,195,319,398	250–577	83.32(83.52)	(ii) ^d	Decomp.
9	[CuL(OAc) ₂].2H ₂ O	38,57	30–85	9.65(9.6) ^c	(i) ^b	–EtOH
		294,329	135–660	82.38(83.88)	(ii) ^d	Decomp.
11	[RuLCl ₃ (H ₂ O)].EtOH	52	30–85	9.5(8.8) ^c	(i) ^a	–2H ₂ O
		345,435	230–295	17.67(17.76)	(ii) ^d	–2(OAc)
12	[PdLCl ₂].1½H ₂ O	48	295–400	65.04(65.35)	(ii) ^d	Completion of decomp.
		271, 362,464	230–353	11.9(12.71) ^c	(ii) ^d	–CuO
11	[RuLCl ₃ (H ₂ O)].EtOH	52	30–125	8.86(8.32)	(i) ^{a+b}	–(EtOH + H ₂ O)
		345,435	260–435	73.82 (74.32)	(ii) ^d	Decomp.
12	[PdLCl ₂].1½H ₂ O	48	30–102	17.32(17.36) ^c	(i) ^a	–½Ru ₂ O ₃
		271, 362,464	230–353	19.35(19.25)	(ii) ^d	–(Cl ₂ + 2CO))
12	[PdLCl ₂].1½H ₂ O	48	353–483	57.13(55.85)	(ii) ^d	Completion of decomp.
		271, 362,464	at 483	19.4 (20.2) ^c	(ii) ^d	–PdO

^a dehydration.^b desolvation.^c final product percent.^d decomposition.**Fig. 1.** The EI mass spectrum of ligand, L.

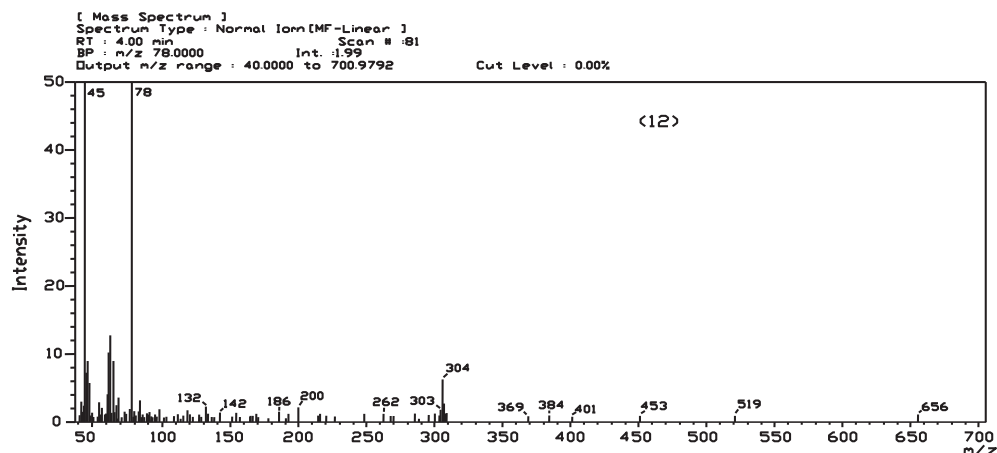


Fig. 2. The ESI mass spectrum of Pd(II) complex (12).

$m/z = 625.5, 654$). The mass spectra of the complexes also show important fragment ions at m/z 63[Cu], 92[Cu(CN)]⁺, 167[Cu(C₇H₄N)]⁺, 194[Cu(C₈H₄ONH)]⁺, 285[Cu(C₁₄H₈ON₂ + H)]⁺, 319[Cu(C₁₄H₈O₃N₂ + H)]⁺, 475[Cu(C₂₄H₁₈O₃N₄ + H)]⁺, 490[Cu(C₂₄H₁₈O₄N₄)]⁺, 532[Cu(C₂₆H₂₀O₅N₄)]⁺, 626[CuLCl₂]H₂O + ½EtOH for complex (6), m/z at 78[C₆H₄ + H]⁺, 200[Pd(C₆H₄O)]⁺, 304[Pd(C₁₂H₁₀N₂O) + 2H]⁺, 519[Pd(C₂₄H₁₈N₄O₃) + H]⁺, 656[PdLCl₂] ½H₂O for complex (12), respectively.

Electronic spectra and magnetic measurements

The electronic spectra of the complexes were recorded in DMF solution. The absorption bands displayed by the complexes as well as the room temperature effective magnetic moment values (μ_{eff} B.M.) are listed in Table 3. The complexes exhibit the high energy bands in the range 450–490 nm which are attributed to the LMCT.

Iron(II) and cobalt(II) complexes

The electronic absorption spectrum of Fe(II) complex (1) exhibits a broad peak at 530 nm, that is assigned to ${}^5T_{2g} \rightarrow {}^5E_g$ transition, suggesting distorted octahedral geometry around Fe(II) ion [40–42]. This finding was further emphasized by the measured magnetic moment (4.76 B.M.), indicating octahedral geometry [40,43]. The electronic absorption spectrum of Co(II) complex (2) exhibits a broad band at 520 nm corresponding to ${}^4T_{1g}(F) \rightarrow {}^4A_{2g}(F)$ transition, which is compatible well with octahedral geometry [44,45]. The magnetic moment value of the Co(II) complex (2) measured at room temperature is found to be 4.99 B.M., which lie in the range (4.80–5.20 B.M.), showing that it has three unpaired electrons and high-spin octahedral configuration [7,44].

Nickel(II) complexes

The electronic absorption spectra of Ni(II) complexes (3–5) display band in the range 540–520 nm which is assigned to ${}^3A_{2g}(F) \rightarrow {}^3T_{1g}(P)$ transition indicating octahedral geometry [45,46]. The magnetic moment of the nickel complexes at room temperature lie in the range 2.1–2.8 B.M. These values agree with the presence of Ni(II) ion in octahedral geometry [45].

Copper(II) complexes

The electronic spectra of the Cu(II) complexes (7,8) exhibit a strong broad band centered at 530–520 nm. The broadness of the

band indicates that the three transitions ${}^2B_{1g} \rightarrow {}^2A_{1g}(v_1)$; ${}^2B_{1g} \rightarrow {}^2B_{2g}(v_2)$, and ${}^2B_{1g} \rightarrow {}^2E_g(v_3)$, which are of similar energy, give rise to only one broad absorption band. The broadness of the band may be due to dynamic Jahn–Teller distortion [45,47–49]. The electronic spectra of the copper(II) complexes (6,9,10) show intensive bands at 700 and 530–500 nm, could be assigned to ${}^2B_{1g} \rightarrow {}^2B_{2g}$, and ${}^2B_{1g} \rightarrow {}^2E_g$ transitions, respectively. This indicates the possibility of square planar geometry of copper(II) complexes [50,51]. The geometry of the Cu(II) complexes is further supported by the magnetic moment values (2.05–2.1 B.M., Table 3). These values correspond to one unpaired electron and indicate that these complexes are monomeric in nature and metal–metal interaction is absent [44].

Ruthenium(III) complex

The electronic absorption spectrum of Ru(III) complex (11) exhibits band at 550 nm. This band is assigned to ${}^2T_{2g} \rightarrow {}^4T_{1g}$ transition [52–54]. The position of the absorption band as well as the magnetic susceptibility measurements (1.88 B.M.) indicate the presence of one unpaired electron and confirm a low-spin octahedral configuration [52].

Palladium(II) complex

The electronic spectrum of Pd(II) complex (12) displays two d–d bands at 600 and 440 nm which may be assigned to ${}^1A_{1g} \rightarrow {}^1A_{2g}$ and ${}^1A_{1g} \rightarrow {}^1B_{1g}$ transitions, respectively. The coordination of the chloride to the square-planar bivalent palladium center is confirmed by its non-electrolytic nature in DMF solution. The electronic spectrum indicates square-planar geometry around the palladium(II) ion [34,50,55] which is further confirmed by its diamagnetic nature.

EPR spectroscopic studies

The solid state EPR spectra of the copper(II) complexes (6–10) (Figs. 3a and 3b) were recorded at room temperature on the X-band frequency 9.719 GHz. The EPR parameters are listed in Table 4. All complexes give axial spectra, analysis of spectra gives $g_{\parallel} = 2.16$ –2.23 and $g_{\perp} = 2.02$ –2.04. The trend $g_{\parallel} > g_{\perp} > 2.0023$ suggests $d_{x^2-y^2}$ ground state for the Cu(II) ion [8,44,45]. Complexes (6,9,10) show hyperfine spectral lines at the lower field, the g_{\parallel} , g_{\perp} , A_{\parallel} , A_{\perp} values have been estimated. The g_{\parallel} values of all complexes are found to be less than 2.3 indicating a considerable covalence character in copper–ligand bond [56]. In addition, the

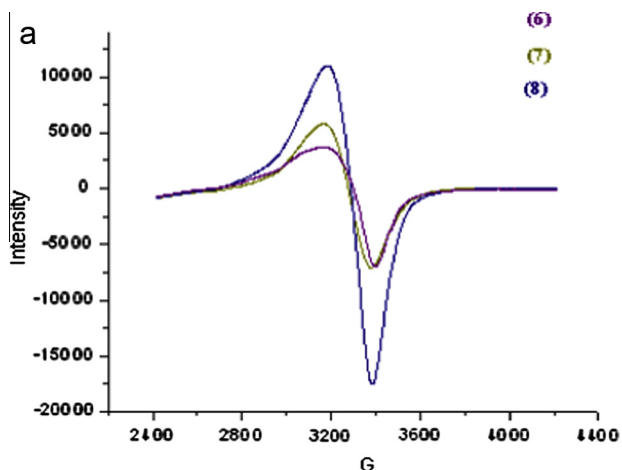


Fig. 3a. EPR spectra of complexes (6–8) as polycrystalline sample at RT.

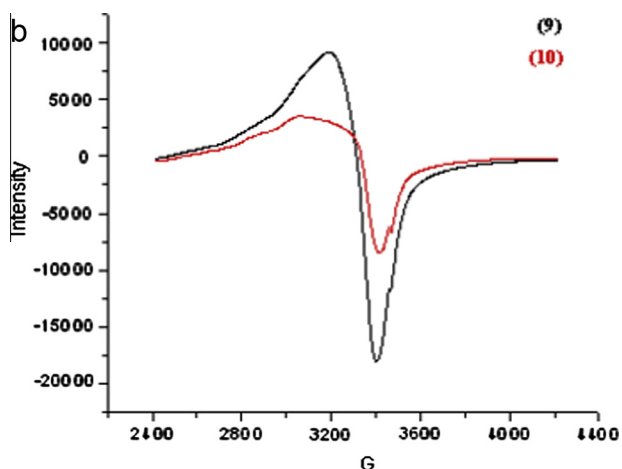


Fig. 3b. EPR spectra of complexes (9,10) as polycrystalline sample at RT.

exchange coupling interaction between two copper centers is explained by Hathaway expression [57], $G = g_{\parallel} - 2.0023/g_{\perp} - 2.0023$. The values of G (6.6–4.28) in these complexes are >4.0 and therefore, the local tetragonal axes are aligned parallel or only slightly misaligned and there is no exchange interaction between copper centers in the polycrystalline compound.

The empirical factor $f = g_{\parallel}/A_{\parallel}$, is an index of tetragonal distortion and its value depends on the nature of the coordinated atom. The value of f from 105 to 135 cm indicates square-planar structures whereas larger values reveal tetragonally distorted complexes [58]. The calculated f values for complexes (6,9,10) (Table 4) fall in the range 116.9–128.5 cm, indicating square planar structure. The EPR parameters and the energies of d–d transitions were used to calculate the bonding parameters α^2 , β^2 and γ^2 which may be regarded as measured of the covalence of the in-plane σ bonds, in-plane and out-of-plane π bonds, respectively [59]. The in-plane σ bonding parameter α^2 , was calculated using the following equations [56,60]: $\alpha^2 = A_{\parallel}/0.036 + (g_{\parallel} - 2.0023) + 3/7(g_{\perp} - 2.0023) + 0.04$. The observed values of α^2 (0.67–0.73) are less than unity, which indicate that the M–L bonds in complexes are partially ionic and partially covalent in nature. Significant information about the nature of bonding in the copper(II) complexes can also be derived from the magnitude of $K_{\parallel} = \alpha^2\beta^2$ and $K_{\perp} = \alpha^2\gamma^2$ which are the parallel and perpendicular components of orbital reduction factor, and were estimated from the expression, $K_{\parallel}^2 = (g_{\parallel} - 2.0023)\Delta_2/8\lambda_0$, $K_{\perp}^2 = (g_{\perp} - 2.0023)\Delta_3/2\lambda_0$,

where λ_0 represents the one electron spin–orbit coupling constant for the free ion and equal to -828 cm^{-1} , $\Delta_2 = {}^2B_{1g} \rightarrow {}^2B_{2g}$, $\Delta_3 = {}^2B_{1g} \rightarrow {}^2E_g$. For pure σ -bonding, $K_{\parallel} \approx K_{\perp} \approx 0.77$, for in-plane π -bonding $K_{\parallel} < K_{\perp}$ and for out-of-plane π -bonding $K_{\parallel} > K_{\perp}$. For complex (9) $K_{\parallel} < K_{\perp}$ indicating in-plane π -bonding, the observed K_{\parallel} and K_{\perp} values for the complexes (6,10) are in agreement with the relation $K_{\parallel} > K_{\perp}$ which is in agreement with the presence of out of plane π -bonding [61,62]. The low values of K (0.365–0.602) indicate the covalent nature of the complexes. Also the values of bonding parameters α^2 , β^2 , γ^2 indicate in-plane π -bonding and in-plane σ bonding.

Thermal studies

In order to give more insight into the structure and thermal stabilities of the ligand and its complexes, the thermal behavior has been carried out using thermogravimetry (TG/DTG) technique. The thermogravimetric studies have been made in the temperature range RT–800 °C. The nature of proposed chemical change with temperature and the percent of metal oxide obtained are given in Table 5. The results obtained from thermogravimetric analysis [63–67] were in agreement with the suggested theoretical formulae from the elemental analyses. The thermal behavior of perchlorate complex (10) has not been investigated, due to its explosive nature.

Ligand

The TGA curve of the ligand shows weight loss of 4.13% (Calc. 4.00%) in the temperature range of 30–100 °C. The DTG peak recorded at 52 °C reflects the loss of one water molecule per ligand molecule. Also the TG curve shows one decomposition step in the temperature range 200–650 °C.

Complexes

Iron(II) and cobalt(II) complexes

The TG curves of Fe(II) and Co(II) complexes (1,2) (Fig. 4) show weight loss in the temperature range 30–150 °C (Calc./Found% 3.12/3.06; 5.43/5.35) associated with one DTG peak at 42,49 °C that was assigned to loss of one or two molecules of water of crystallization for complexes (1,2), respectively. The TG/DTG curves exhibit gradual decomposition at a temperature range 147–150 °C, leaving Fe_2O_3 , Co_2O_3 as final residue.

Nickel (II) complexes

For Ni(II) complexes (3–5), the TG curves show weight loss in the temperature range 30–148 °C (Calc./Found% 7.57/7.66; 3.51/3.2; 7.9/7.43) associated with one DTG peak at 53–61 °C. That was assigned to loss of solvent of crystallization in one step (Table 5). On further heating the thermograms register a plateau region, corresponding to Ni for complexes (3,4), NiO for complex (5), respectively.

Copper(II) complexes

The TG/DTG curves of Cu(II) complexes (6–9) (Fig. 4) show weight loss from room temperature up to 132 °C, associated with one DTG peak, that was attributed to loss of solvent of crystallization on one step (Table 5). On further heating the complexes decomposed at 135–250 °C. The thermogram of complex (9) shows two steps of decomposition. The first one (230–295 °C) is due to the loss of 2(OAc) (Calc./Found%; 17.67/17.76), the second one (295–400 °C) involves the completion of the decomposition process. The thermograms register a plateau region, corresponding to Cu for complexes (6–8), CuO for complex (9), respectively.

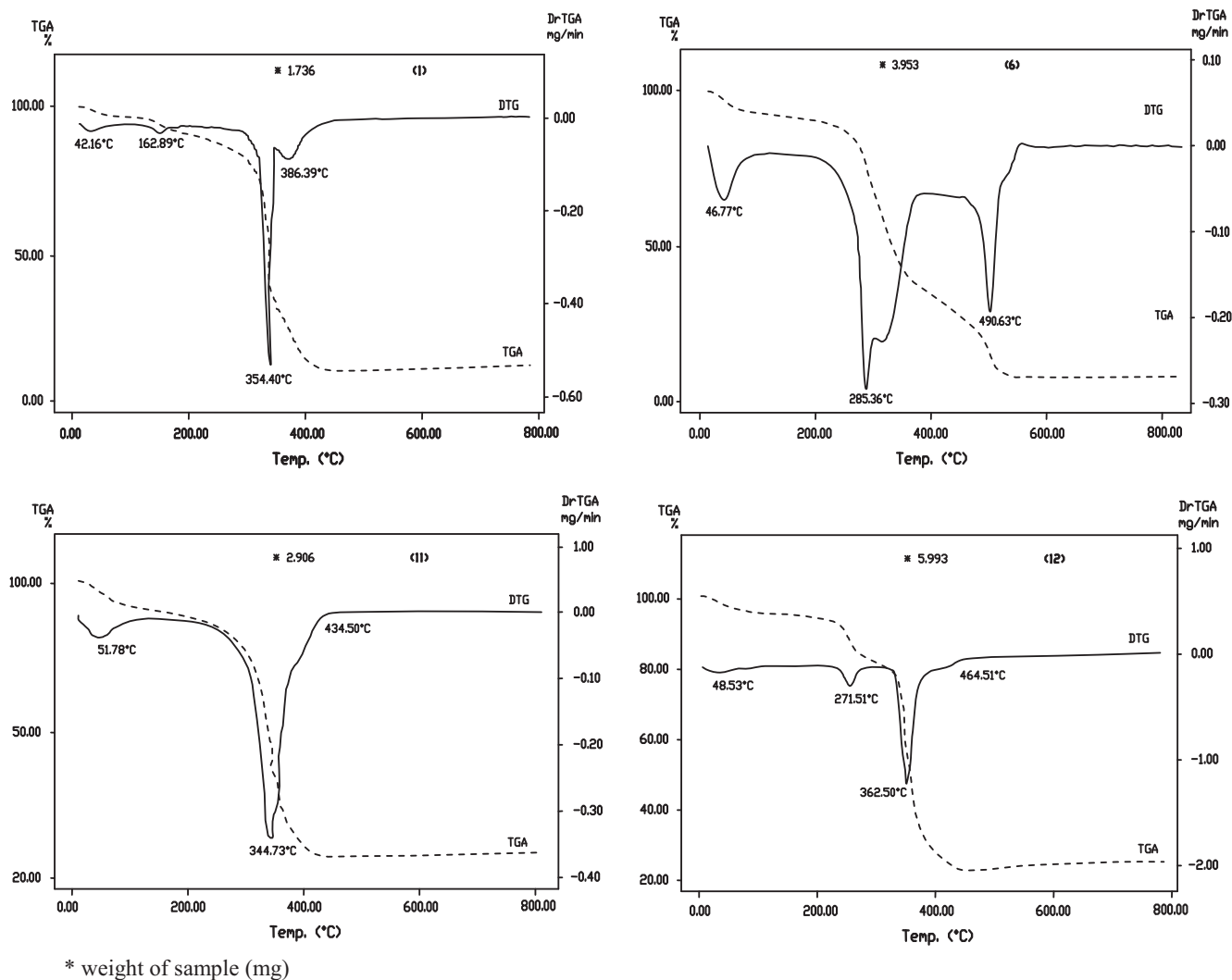


Fig. 4. TG/DTG curves of the complexes (1,6,11,12).

Table 6
Kinetic and thermodynamic data of complexes (6,7,9,11,12).

No	Complex	D.T. (K)	A (S ⁻¹)	S [‡] (J mol ⁻¹ K ⁻¹)	E [‡] (kJ mol ⁻¹)	H [‡]	G [‡]	C _s	^a R ²
6	[CuCl ₂].H ₂ O.½EtOH	493–823	8.094E ⁵	-16.558	22.820	17.844	27.74	0.34	0.98
7	[CuLBr(OH)].EtOH	523–850	5.373E ⁶	-14.839	47.902	41.978	52.543	0.38	0.98
9	[CuL(OAc) ₂].2H ₂ O	503–673	1.069E ⁶	-16.305	44.6	39.49	49.501	0.37	0.97
11	[RuCl ₃ (H ₂ O)].EtOH	533–708	2.317E ⁵	-17.547	13.853	8.608	19.66	0.39	0.97
12	[PdCl ₂].1½H ₂ O	503–756	4.927E ⁴	-19.4348	9.178	3.8032	16.358	0.28	0.98

^a R²: Correlation coefficient.

Ruthenium(III) and palladium(II) complexes

The TG curves of Ru(III) and Pd(II) complexes (11,12) (Fig. 4) show weight loss in the temperature range 30–125 °C, (Calc./Found% 8.86/8.32; 4.12/4.7) associated with one DTG peak at 52, 48 °C, that was assigned to loss of solvent of crystallization (Table 5), the TG/DTG curve of complex (11) exhibits gradual decomposition at 260 °C, remaining Ru₂O₃ as final residue. Complex (12) shows two decomposition stages. The first one, in the temperature range 230–353 °C is due to loss of chlorine molecule together with two molecules of carbon monoxide (weight loss; Calc./Found%; 19.35/19.25). The second one involves the completion of the decomposition process, remaining PdO as final residue [1,66].

Kinetic and thermodynamic parameters for complexes (6,7,9,11,12)

The kinetic and thermodynamic parameters of the decomposition stages of the desolvated complexes (6,7,9,11,12) were determined from TGA thermogram using the Coats–Redfern equation [68]. The Horowitz and Metzger [69] equation $C_s = (n)^{1/n}$ was used for the determination of the value of the reaction order, and given by $C_s = \frac{m_s - m_\infty}{m_0 - m_\infty}$, where C_s is the weight fraction of the substance present at DTG peak temperature T_s , m_s is the remaining weight at T_s , m_0 and m_∞ are the initial and final weights of the substance, respectively. The estimated values of C_s for the thermal decomposition of the desolvated complexes were found in the range of 0.28–0.39 (Table 6). This indicates that the decomposition follows first order kinetic [70]. So, the values of the activation

Table 7
Lethal concentration (IC₅₀) of the ligand and some of its metal complexes on MCF-7 and HepG2.

No	Compound	IC ₅₀ (μg/mL) ^a	
		MCF-7	HepG2
	L = C ₂₆ H ₁₈ N ₄ O ₄ ·H ₂ O	13	26
1	[FeLCl(OH)]·H ₂ O	2.5	8.33
3	[NiLCl(OH)]·EtOH	2.7	(Na) ^b
6	[CuLCl ₂]·H ₂ O·½EtOH	2.3	24.5
11	[RuLCl ₃ (H ₂ O)]·EtOH	2.39	30.5
12	[PdLCl ₂]·1½H ₂ O	2.27	31.1

^a IC₅₀ is the concentration of compound (in μg/mL) that inhibits a proliferation rate of the tumor cells by 50% as compared to control untreated cells.

^b Na = has no activity.

energy E^* , Arrhenius constant A , the activation entropy S^* , the activation enthalpy H^* and the free energy of activation G^* are calculated by applying Coats–Redfern equation for $n = 1$:

$$\log \left[\frac{-\log(1-x)}{T^2} \right] = \log \frac{AR}{\theta E^*} \left[1 - \frac{2RT}{E^*} \right] - \frac{E^*}{2.303RT} \quad (1)$$

where x is the fraction decomposed, R : is the gas constant and θ is the heating rate. Since $(1-2RT/E^*) \approx 1$, a plot of the left-hand side of Eq. (1) against $1/T$ gives a straight line from its slope and intercept, E^* and A were calculated. The entropy of activation S^* , enthalpy of activation H^* and the free energy change of activation G^* were calculated using the following equations. $S^* = R \ln(Ah/kT)$, $H^* = E^* - RT$ and $G^* = H^* - TS^*$. The calculated kinetic and thermodynamic values are summarized in Table 6. The high values of E^* reveal high stability of the chelates. Since $H^* > 0$ the reactions are endothermic. The reaction for which G^* is positive and S^* is negative considered as non-spontaneous reactions. The entropy of activation was found to have negative values in the complexes, indicating that the activated complex has a more ordered structure than the corresponding reactant [71]. The correlation coefficients of the Arrhenius plots of the thermal decomposition steps were found to lie in the range 0.98–0.97 showing a good fit with linear function.

On the basis of elemental analyses, molar conductance measurements, magnetic susceptibilities, different spectra and thermal data the suggested structures for the complexes (1–12) are given in Scheme 2.

Biological activity

The results of the *in vitro* cytotoxic activity were expressed as IC₅₀ (the concentration of the compound in μg/mL that inhibits proliferation of the cells by 50% as compared to the untreated control cells) are given in Table 7. The ligand shows IC₅₀ value of 13, 26 μg/mL towards human breast cancer cell lines (MCF-7) and human hepatocarcinoma cells (HepG2), respectively and that for some selected complexes (1,6,11,12) was in the range of 2.27–2.7 μg/mL towards the former cells and 8.0–31.1 μg/mL towards the latter one, respectively. Shier [72] suggested that compounds exhibiting IC₅₀ values more than 10–25 μg/mL indicate weak cytotoxic activities while compounds with IC₅₀ values less than 5 μg/mL are considered to be very active. Those having intermediate values ranging from 5 to 10 μg/mL are classified as moderately active. Accordingly, the tested complexes (IC₅₀ = 2.27–2.70 μg/mL) are considered to be very active towards human breast cancer cell lines. The results also show that Pd(II) complex (12) showed highest cytotoxic activity towards human breast cancer cell lines, (IC₅₀ value = 2.27 μg/mL). Fe(II) complex (1) (IC₅₀ value = 8.33 μg/mL) showed highest cytotoxic activity towards human hepatocarcinoma cells. The enhanced activity of the investigated complexes agrees well with and better than the documented activity of

similar metal complexes as antitumor agents [2,61,73–75]. The enhanced activity may be attributed to the increase in conjugation in the ligand moiety on complexation [76]. The type of metal ions may be another reason for their different anticancer activity. These compounds seem to be promising as an anticancer agent towards human breast cancer cell lines because of their high cytotoxic activity. The active sequence of the ligand and its complexes follows the trend:

Pd(II) > Cu(II) > Ru(III) > Fe(II) > Ni(II) > L for MCF-7 cells,

Fe(II) > Cu(II) > L > Ru(III) > Pd(II) for HepG2 cells

Conclusions

We have presented the synthesis and characterization of a novel tetraamide (N₄) macrocyclic ligand and some of its transition metal complexes (1–12). The physicochemical and spectroscopic data confirmed the composition and the structure of the newly obtained compounds. Spectral, magnetic, thermal studies lead to the conclusions that:

1. The ligand behaves as neutral quadridentate or neutral bidentate one.
2. The metal complexes exhibited octahedral or square planar geometry.
3. EPR studies indicate the covalent nature of the complexes.
4. The results of the *in vitro* anticancer activity against breast cancer cell line (MCF7), hepatocarcinoma cancer cells (HepG2) showed that the ligand as well as its complexes is potent anticancer agents, which have potential to develop as anticancer drugs. Besides, the cytotoxicity of the complexes is higher than that of the ligand, which implies an increase in the antitumor activity with coordination.

Acknowledgements

The authors would like to thank Dr. Mahmoud Moawad, Pathology Department, National Cancer Institute, Cairo University, Cairo, Egypt, for his help with the *in vitro* anticancer activity.

Appendix A. Supplementary material

Supplementary data associated with this article can be found, in the online version, at <http://dx.doi.org/10.1016/j.saa.2014.11.015>.

References

- [1] H.A. El-Boraey, Spectrochim. Acta A 97 (2012) 255–262.
- [2] H.A. El-Boraey, S.M. Emam, D.A. Tolan, A.M. El-Nahas, Spectrochim. Acta A 78 (2011) 360–370.
- [3] D.P. Singh, V. Malik, K. Kumar, C. Sharma, K.R. Aneja, Spectrochim. Acta A 76 (2010) 45–49.
- [4] S. Rani, S. Kumar, S. Chandra, Spectrochim. Acta A 118 (2014) 244–250.
- [5] R. Kumar, I. Masih, N. Fahmi, Spectrochim. Acta A 101 (2013) 100–106.
- [6] I. Masih, N. Fahmi, Spectrochim. Acta A 79 (2011) 940–947.
- [7] U. Kumar, S. Chandra, J. Saudi Chem. Soc. 15 (2011) 187–193.
- [8] H.A. El-Boraey, A.A. Serag El-Din, Spectrochim. Acta A 132 (2014) 663–671.
- [9] A.A. Khandar, S.A. Hosseini-Yazdi, M. Khatamian, S.A. Zarei, Polyhedron 29 (2010) 995–1000.
- [10] D.P. Singh, K. Kumar, C. Sharma, Spectrochim. Acta A 75 (2010) 98–105.
- [11] L.K. Gupta, S. Chandra, Spectrochim. Acta A 65 (2006) 792–796.
- [12] Z. Qi, Q. Yuan, Shu-An Li, T. Okamura, K. Cai, W. Sun, N. Ueyama, J. Mol. Struct. 973 (2010) 104–115.
- [13] B.K. Daszkiewicz, R. Bilewicz, K. Wóznik, Coord. Chem. Rev. 254 (2010) 1637–1660.
- [14] S.A. Zarei, A. Khandar, M. Khatamian, S.A. Hosseini-Yazdi, I. Dechamps, E. Guillon, M. Piltan, Inorg. Chim. Acta 394 (2013) 348–352.

- [15] M. Tyagi, S. Chandra, J. Akhtar, D. Chand, *Spectrochim. Acta A* 118 (2014) 1056–1061.
- [16] M.C. Fernández-Fernández, R.B. la Calle, A. Macías, L.V. Matarranz, P. Pérez-Lourido, *Polyhedron* 27 (2008) 2301–2308.
- [17] G. Ferraudi, J.C. Canales, B. Kharisov, J. Costamagna, J.G. Zagal, G. Cardenas-Jirónand, M. Paez, *J. Coord. Chem.* 58 (1) (2005) 89–109.
- [18] A. Chaudhary, N. Bansal, A. Gajraj, R.V. Singh, *Inorg. Biochem.* 96 (2003) 393–400.
- [19] M. Numata, K. Hiratani, Y. Nagawa, H. Houjou, S. Masubuchi, S. Akabori, *New J. Chem.* 26 (2002) 503–507.
- [20] D.P. Singh, K. Kumar, C. Sharma, *Eur. J. Med. Chem.* 44 (2009) 3299–3304.
- [21] N. Raja, M.U. Raja, R. Ramesh, *Inorg. Chem. Commun.* 19 (2012) 51–54.
- [22] M. Munjal, S. Kumar, S.K. Sharma, R. Gupta, *Inorg. Chim. Acta* 377 (2011) 144–154.
- [23] C.W. Yeh, K.H. Chang, C.Y. Hu, W. Hsu, J.D. Chen, *Polyhedron* 31 (2012) 657–664.
- [24] N. Raman, R. Rajakumar, *Spectrochim. Acta A* 120 (2014) 428–436.
- [25] A. Mohamadou, J. Moreau, L. Dupont, E. Wenger, *Inorg. Chim. Acta* 383 (2012) 267–276.
- [26] A.K. Sharma, S. Biswas, S.K. Barman, R. Mukherjee, *Inorg. Chim. Acta* 363 (2010) 2720–2727.
- [27] A.A.A. Mohamed, *Coord. Chem. Rev.* 254 (2010) 1918–1947.
- [28] S.J. Swamy, B. Veerapratap, D. Nagaraju, K. Suresh, P. Someswar, *Tetrahedron* 59 (2003) 10093–10096.
- [29] J. Bassett, R.C. Denney, G.H. Jeffery, J. Mendham, *Vogel's Textbook of Quantitative Inorganic Analysis Including Elementary Instrumental Analysis*, fourth ed., Longman Group, London, 1978, pp. 316–322.
- [30] T.S. West, *Complexometry with EDTA and Related Reagents*, third ed., DBH Ltd., Pools, 1969.
- [31] P. Skehan, R. Storeng, D. Scudiero, A. Monks, J. McMahon, D. Vistica, J.T. Warren, H. Bokesch, S. Kenney, M.R. Boyd, *J. Natl. Cancer Inst.* 82 (1990) 1107–1112.
- [32] W.J. Geary, *Coord. Chem. Rev.* 7 (1971) 81–122.
- [33] S. Chandra, L.K. Gupta, *Spectrochim. Acta A* 60 (2004) 1751–1761.
- [34] S. Chandra, S. Raizada, S. Rani, *Spectrochim. Acta A* 71 (2008) 720–724.
- [35] S. Chandra, L.K. Gupta, *Spectrochim. Acta A* 62 (2005) 1125–1130.
- [36] S. Chandra, M. Pundir, *Spectrochim. Acta A* 69 (2008) 1–7.
- [37] S.J. Swamy, E.R. Reddy, D.N. Raju, S. Jyothi, *Molecules* 11 (2006) 1000–1008.
- [38] H.A. El-Boraey, R.M. Abdel-Raham, E.M. Atia, K.H. Hilmy, *Cent. Eur. J. Chem.* 8 (2010) 820–833.
- [39] S. Sreedaran, K.S. Bharathi, A.K. Rahiman, K. Rajesh, G. Nirmala, L. Jagadish, V. Kaviyaranan, V. Narayanan, *Polyhedron* 27 (2008) 1867–1874.
- [40] A.A. Soliman, M.A. Amin, A.A. El-Sherif, S. Ozdemir, C. Varlikli, C. Zafer, *Dyes Pigm.* 99 (2013) 1056–1064.
- [41] Z.G. Gu, J.J. Na, F.F. Bao, X.X. Xu, W. Zhou, C.Y. Pang, Z. Li, *Polyhedron* 51 (2013) 186–191.
- [42] T.V. Serebryanskaya, L.S. Ivashkevich, A.S. Lyakhov, P.N. Gaponik, O.A. Ivashkevich, *Polyhedron* 29 (2010) 2844–2850.
- [43] U. Ray, D. Banerjee, J.C. Liou, C.N. Lin, T.H. Lu, C. Sinha, *Inorg. Chim. Acta* 358 (2005) 1019–1026.
- [44] M. Shakir, A. Abbasi, M. Azam, A.U. Khan, *Spectrochim. Acta A* 79 (2011) 1866–1875.
- [45] M. Shebl, S.M.E. Khalil, F.S. Al-Gohani, *J. Mol. Struct.* 980 (2010) 78–87.
- [46] S. Ilhan, H. Temel, *J. Mol. Struct.* 891 (2008) 157–166.
- [47] G.G. Mohamed, N.A. Ibrahim, H.A.E. Attia, *Spectrochim. Acta A* 72 (2009) 610–615.
- [48] S. Budagumpi, M.P. Sathisha, N.V. Kulkarni, G.S. Kurdekar, V.K. Revankar, *J. Incl. Phenom. Macrocycl. Chem.* 66 (2010) 327–333.
- [49] S.G. Kang, J. Song, J.H. Jeong, *Inorg. Chim. Acta* 357 (2004) 605–610.
- [50] B. Geeta, K. Shrivankumar, P.M. Reddy, E. Ravikrishna, M. Sarangapani, K.K. Reddy, V. Ravinder, *Spectrochim. Acta A* 77 (2010) 911–915.
- [51] Abdel-Nasser M.A. Alaghaz, A.G. Al-Sehemi, T.M. EL-Gogary, *Spectrochim. Acta A* 95 (2012) 414–422.
- [52] N. Raja, R. Ramesh, *Spectrochim. Acta A* 75 (2010) 713–718.
- [53] A.K. Devi, R. Ramesh, *Spectrochim. Acta A* 117 (2014) 138–143.
- [54] S. Rani, S. Kumar, S. Chandra, *Spectrochim. Acta A* 78 (2011) 1507–1514.
- [55] A. Budakoti, M. Abid, A. Azam, *Eur. J. Med. Chem.* 42 (2007) 544–551.
- [56] D. Kivelson, R. Neiman, *J. Chem. Phys.* 35 (1961) 149–155.
- [57] B.J. Hathaway, D.E. Billing, *Coord. Chem. Rev.* 5 (1970) 143–207.
- [58] U. Sakagushi, A.W. Addison, *J. Chem. Soc. Dalton Trans.* (1979) 600–608.
- [59] A.L. Sharma, I.O. Singh, M.A. Singh, H.R. Singh, *Trans. Met. Chem.* 26 (2001) 532–537.
- [60] A.H. Maki, B.R. McGarvey, *J. Chem. Phys.* 29 (1958) 35–38.
- [61] W.H. Mahmoud, G.G. Mohamed, M.M.I. El-Dessouky, *Int. J. Electrochem. Sci.* 9 (2014) 1415–1438.
- [62] T. Rosu, E. Pahontu, C. Maxim, R. Georgescu, N. Stanica, G.L. Almjan, A. Gulea, *Polyhedron* 29 (2010) 757–766.
- [63] A.M. Donia, H.A. El-Boraey, M.F. El-Samalehy, *J. Therm. Anal. Calorim.* 73 (2003) 987–1000.
- [64] M.I. Ayad, H.A. El-Boraey, *Int. J. Chem. Technol. Res.* 6 (1) (2014) 266–275.
- [65] H.A. El-Boraey, F.A. El-Saied, S.A. Aly, *J. Therm. Anal. Calorim.* 96 (2009) 599–606.
- [66] H.A. El-Boraey, S.A. Aly, *Synth. React. Inorg. Met. Org. Nano Chem.* 43 (2013) 1–9.
- [67] H.A. El-Boraey, *J. Therm. Anal. Calorim.* 81 (2005) 339–346.
- [68] A.W. Coats, J.P. Redfern, *Nature* 20 (1964) 68–122.
- [69] H.H. Horowitz, G. Metzger, *J. Anal. Chem.* 35 (1963) 1464–1468.
- [70] M. Nathg, P. Arora, *Synth. React. Inorg. Met. Org. Chem.* 23 (1993) 1523–1545.
- [71] H.A. El-Boraey, A.M. Donia, M.F. El-Samalehy, *J. Anal. Appl. Pyrol.* 73 (2005) 204–211.
- [72] W.T. Shier, *Mammalian Cell Culture on \$5 a Day: a Laboratory Manual of Low Cost Methods*, University of the Philippines, Los Banos, 1991.
- [73] W.J. Song, J.P. Cheng, D.H. Jiang, L. Guo, M.F. Cai, H.B. Yang, Q.Y. Lin, *Spectrochim. Acta A* 121 (2014) 70–76.
- [74] K. Abdi, H. Hadadzadeh, M. Weil, M. Salimi, *Polyhedron* 31 (2012) 638–648.
- [75] J.L. García-Giménez, J. Hernández-Gil, A. Martínez-Ruiz, A. Castiñeiras, M. Liu-González, F.V. Pallardó, J. Borrás, G.A. Piña, *J. Inorg. Biochem.* 121 (2013) 167–178.
- [76] Q. Xiao-Yang, L. Su-Zhi, S. An-Ran, L. Qian-Qian, Z. Bin, *Chinese J. Struct. Chem.* 31 (4) (2012) 555–561.